European Journal of Mechanics A/Solids 36 (2012) 204–212

Contents lists available at SciVerse ScienceDirect

European Journal of Mechanics A/Solids

journal homepage: www.elsevier.com/locate/ejmsol

Free vibration analysis of moderately thick trapezoidal symmetrically laminated plates with various combinations of boundary conditions

M. Zamani, A. Fallah [1], M.M. Aghdam*

Department of Mechanical Engineering, Amirkabir University of Technology, 424 Hafez Avenue, Tehran 15875, Iran

A R T I C L E I N F O

Article history:
Received 27 December 2011
Accepted 18 March 2012
Available online 30 March 2012

Keywords:
Free vibration analysis
Trapezoidal and skew plate
Generalized differential quadrature

A B S T R A C T

In this study, free vibration analysis of moderately thick symmetrically laminated general trapezoidal plates with various combinations of boundary conditions is investigated. The governing partial differential equations and boundary conditions for trapezoidal plate are obtained using first order shear deformation theory (FSDT) together with proper transformation from Cartesian system into trapezoidal coordinates. Generalized differential quadrature (GDQ) method is then employed to obtain solutions for the governing equations. Results of the GDQ method are compared and validated with available results in the literature which show accuracy and fast rate of convergence of the method. Effect of various parameters such as geometry, thickness, boundary condition and lay-up configuration on the natural frequency of trapezoidal and skew plates is investigated through several examples. It is also shown that the method can be used for analysis of triangular plates as special case of trapezoidal geometry with the same performance and convergence.

1. Introduction

Composite laminated plates with high stiffness and strength to weight ratios are increasingly used in many engineering fields such as civil, marine and aerospace structures. Due to huge application of laminated plates in different fields for more efficient design, it is necessary to study their dynamic behavior. Most studies for dynamic analysis of laminated plates are mainly concerned with rectangular or annular/circular laminated plates (Rao and Meyer Piening, 1990; Rajalingham et al., 1996; Khdeir, 1988; Xiang, 2002; Liew and Haung, 2003; Zhou et al., 2003; Kang et al., 2005; Yalcin et al., 2009; Ferreira et al., 2011). On the other hand, however, plates of nonrectangular shape such as trapezoidal and skew are common industrial elements in many engineering fields like air craft wings, ship substructures, bridge entrance and vehicle bodies. A few studies can be found in the literature for free vibration analysis of nonrectangular plates which are mainly limited to isotropic and thin laminated plates. For instance, Ng and Das (1986) used Galerkin method to study free vibration and buckling of thin clamped skew sandwich plates. Ritz method is also used to study the free vibration of thin isotropic and anisotropic skew and trapezoidal plate (Liew and Lam, 1991), thick isotropic skew plate (Liew et al., 1993), symmetrically laminated cantilevered thin trapezoidal plate (Liew, 1992), moderately thick isotropic trapezoidal plate (Kitipornchni et al., 1994), thin symmetrically laminated cantilevered right angular and trapezoidal plate (Qatu, 1994), thick isotropic quadrilateral plates (Dozio and Carrera, 2011) and three dimensional free vibration of cantilevered thick isotropic plates (Zhou et al., 2008). Finite element method is also used to investigate the free vibration of thin isotropic skew plate (Bardell, 1992) and cantilevered isotropic moderately thick trapezoidal plate (McGee and Butalia, 1992) and moderately thick isotropic skew plate (Woo et al., 2003).

Liew et al. (1995) presented an exact expression for the three dimensional free vibration of simply supported isotropic skew plate. Fallah et al. (2011) presented a semi-analytical solution for free vibration analysis of symmetrically laminated thin skew plates with clamped edges using extended Kantorovich method. Malekzadeh and Karami (2005) used the polynomial and harmonic differential quadrature (DQ) method to study free vibration analysis of isotropic moderately thick skew plates. Ferreira et al. (2005) used FSDT and radial basic functions to investigate the free vibration of symmetrically laminated composite rectangular and skew plates.

A few studies can be found in the literature for free vibration analysis of thick laminated trapezoidal plates. For instance, Chen et al. (1999) studied free vibration of cantilevered symmetrically laminated thick trapezoidal plates using *p*-Ritz method incorporating third-order shear deformation theory. Haldar and Manna

* Corresponding author. Tel.: +98 21 64543429; fax: +98 21 66419736.
E-mail addresses: a_fallah@mech.sharif.edu (A. Fallah), aghdam@aut.ac.ir (M.M. Aghdam).

[1] Current address: School of Mechanical Engineering, Sharif University of Technology, Tehran, Iran.

0997-7538/$ – see front matter © 2012 Elsevier Masson SAS. All rights reserved.
doi:10.1016/j.euromechsol.2012.03.004

(2003) presented a high precision shear deformable element for free vibration analysis of thick composite trapezoidal plates. Gürses et al. (2009) studied free vibration analysis of fully clamped and simply supported laminated trapezoidal plates using discrete singular convolution (DSC) method. However, studies related to the free vibration of thick laminated trapezoidal plates are limited to some special boundary conditions such as cantilever, fully clamped and simply supported.

In this study, free vibration analysis of moderately thick symmetrically laminated trapezoidal and skew plates is investigated. Various combinations of simply supported, clamped and free boundary conditions are considered. Equations of motion are obtained based on the first order shear deformation theory (FSDT) in Cartesian coordinates. Then governing equations are transformed into trapezoidal coordinates using mapping techniques and Jacobean matrices. The GDQ method is used to discretize the domain and boundary condition equations. Comparing between the GDQ results and DSC, Ritz and FEM ones shows the accuracy and high rate of convergence of method. Effect of various parameters such as geometry, plates thickness, boundary conditions and lay-up on the dynamic behavior of the skew and trapezoidal plates are investigated through several examples. As an especial case, triangle plate is considered by limiting one edge of trapezoidal length to zero. Results for triangular plates reveal that the method provides reasonably accurate predictions in comparison with finite element code.

2. Governing equations

A trapezoidal plate with thickness h in z direction, two lengths L_x and L_y and two angles α and β in the x–y plane is considered as shown in Fig. 1. The physical domain can be mapped into computational rectangular domain using following transformation:

$$x = \zeta + \eta\cos(\alpha) - \frac{\eta\zeta\sin(\beta-\alpha)}{L_x\sin(\beta)}$$
$$y = \eta\sin(\alpha) \tag{1}$$

Based on the FSDT, the governing equations of motion for free vibration analysis of symmetrically laminated plate in Cartesian coordinate system are (Reddy, 1997):

$$k^2A_{55}\left(\frac{\partial\phi_x}{\partial x}+\frac{\partial^2 w}{\partial x^2}\right)+k^2A_{44}\left(\frac{\partial\phi_y}{\partial y}+\frac{\partial^2 w}{\partial y^2}\right)+k^2A_{45}\frac{\partial\phi_x}{\partial y}+k^2A_{45}\frac{\partial\phi_y}{\partial x}+2k^2A_{45}\frac{\partial^2 w}{\partial x\partial y} = I_0\ddot{w} \tag{2}$$

$$D_{11}\left(\frac{\partial^2\phi_x}{\partial x^2}\right)+D_{12}\left(\frac{\partial^2\phi_y}{\partial x\partial y}\right)+D_{66}\left(\frac{\partial^2\phi_x}{\partial y^2}+\frac{\partial^2\phi_y}{\partial x\partial y}\right)-k^2A_{55}\left(\phi_x+\frac{\partial w}{\partial x}\right)-k^2A_{45}\left(\phi_y+\frac{\partial w}{\partial y}\right)+2D_{16}\frac{\partial^2\phi_x}{\partial x\partial y}+D_{16}\frac{\partial^2\phi_y}{\partial x^2}+D_{26}\frac{\partial^2\phi_y}{\partial y^2} = I_2\ddot{\phi}_x$$

$$D_{66}\left(\frac{\partial^2\phi_y}{\partial x^2}+\frac{\partial^2\phi_x}{\partial x\partial y}\right)+D_{12}\left(\frac{\partial^2\phi_x}{\partial x\partial y}\right)+D_{22}\left(\frac{\partial^2\phi_y}{\partial y^2}\right)-k^2A_{44}\left(\phi_y+\frac{\partial w}{\partial y}\right)+D_{16}\frac{\partial^2\phi_x}{\partial x^2}+D_{26}\frac{\partial^2\phi_x}{\partial y^2}+2D_{26}\frac{\partial^2\phi_y}{\partial x\partial y}-k^2A_{45}\left(\phi_x+\frac{\partial w}{\partial x}\right) = I_2\ddot{\phi}_y$$

where ϕ_x and ϕ_y are the rotations of the middle surface of the plate about the x and y axes, respectively and w is transverse deflection of the middle surface. Furthermore, k^2 is the shear correction factor which is assumed to be 5/6 while other constants are defined as:

$$(A_{ij},B_{ij},D_{ij}) = \int_{-h/2}^{h/2}\left(1,z,z^2\right)\overline{Q}_{ij}^{(k)}dz = \sum_{k=1}^{N}\int_{z_k}^{z_{k+1}}\overline{Q}_{ij}^{(k)}\left(1,z,z^2\right)dz \tag{3}$$

in which $\overline{Q}_{ij}^{(k)}$ are the plane stress-reduced stiffnesses and the detailed definition of them can be found in Reddy (1997).

Various boundary conditions for an arbitrary edge whose normal and tangential directions are denoted by n and s are as (Malekzadeh and Karami, 2005):

Free (F):

$$M_n = 0,\quad Q_n = 0,\quad M_{ns} = 0 \tag{4.1}$$

Simply supported (S):

$$w = 0,\quad \phi_s = 0,\quad M_n = 0 \tag{4.2}$$

Clamped (C):

$$w = 0,\quad \phi_s = 0,\quad \phi_n = 0 \tag{4.3}$$

where M_n and M_{ns} are resultant bending and twisting moments, respectively and Q_n is resultant shear force acting on the boundary in the z direction. Furthermore, ϕ_n and ϕ_s are rotations of the normal to the mid-plane in the plane nz (normal plane) and sz (tangent plane), respectively. These parameters can be defined in Cartesian coordinate as:

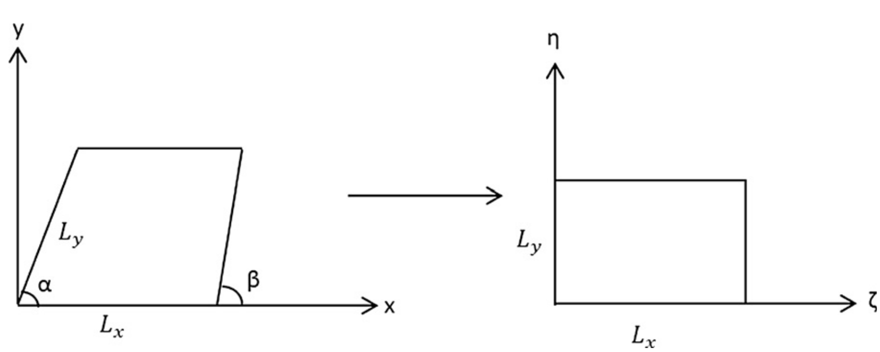

Fig. 1. Physical and computational mapped domain.

$$
\begin{aligned}
\phi_s &= -n_y\phi_x + n_x\phi_y \\
\phi_n &= n_y\phi_y + n_x\phi_x \\
M_n &= M_{xx}n_x^2 + M_{yy}n_y^2 + 2M_{xy}n_xn_y \\
M_{ns} &= n_xn_y(M_y - M_x) + M_{xy}\left(n_x^2 - n_y^2\right) \\
Q_n &= n_xQ_x + n_yQ_y
\end{aligned}
\tag{5}
$$

where n_x and n_y are the x and y components of the vector normal to the edge, respectively and M and Q are resultant moments and shear forces in the Cartesian coordinates which are defined as:

$$
\begin{Bmatrix} M_{xx} \\ M_{yy} \\ M_{xy} \end{Bmatrix} = \begin{bmatrix} D_{11} & D_{12} & D_{16} \\ D_{12} & D_{22} & D_{26} \\ D_{16} & D_{26} & D_{66} \end{bmatrix} \begin{Bmatrix} \dfrac{\partial \phi_x}{\partial x} \\ \dfrac{\partial \phi_y}{\partial y} \\ \dfrac{\partial \phi_y}{\partial x} + \dfrac{\partial \phi_x}{\partial y} \end{Bmatrix}
\tag{6}
$$

$$
\begin{Bmatrix} Q_x \\ Q_y \end{Bmatrix} = k^2 \begin{bmatrix} A_{55} & A_{45} \\ A_{45} & A_{44} \end{bmatrix} \begin{Bmatrix} \phi_x + \dfrac{\partial w}{\partial x} \\ \phi_y + \dfrac{\partial w}{\partial y} \end{Bmatrix}
$$

Derivations in new $\zeta{-}\eta$ coordinate can be related to the derivations in Cartesian coordinate as:

$$
\begin{Bmatrix} \dfrac{\partial V}{\partial x} \\ \dfrac{\partial V}{\partial y} \end{Bmatrix} = [j]^{-1} \begin{bmatrix} \dfrac{\partial V}{\partial \zeta} \\ \dfrac{\partial V}{\partial \eta} \end{bmatrix}
$$

$$
\begin{Bmatrix} \dfrac{\partial^2 V}{\partial x^2} \\ \dfrac{\partial^2 V}{\partial y^2} \\ \dfrac{2\partial^2 V}{\partial x \partial y} \end{Bmatrix} = \left[j^{(2)}\right]^{-1} \begin{Bmatrix} \dfrac{\partial^2 V}{\partial \zeta^2} \\ \dfrac{\partial^2 V}{\partial \eta^2} \\ \dfrac{\partial^2 V}{\partial \zeta \partial \eta} \end{Bmatrix} - \left[j^{(2)}\right]^{-1}\left[j^{(1)}\right][j]^{-1} \begin{Bmatrix} \dfrac{\partial V}{\partial \zeta} \\ \dfrac{\partial V}{\partial \eta} \end{Bmatrix}
\tag{7}
$$

in which V stands for an arbitrary variable and $[j]$,$[j^{(1)}]$ and $[j^{(2)}]$ are defined as:

$$
[j] = \begin{bmatrix} x_{,\zeta} & y_{,\zeta} \\ x_{,\eta} & y_{,\eta} \end{bmatrix} = \begin{bmatrix} 1 - \eta\dfrac{\sin(\beta-\alpha)}{L_x\sin(\beta)} & 0 \\ \cos(\alpha) - \zeta\dfrac{\sin(\beta-\alpha)}{L_x\sin(\beta)} & \sin(\alpha) \end{bmatrix}
$$

$$
\left[j^{(1)}\right] = \begin{bmatrix} x_{,\zeta\zeta} & y_{,\zeta\zeta} \\ x_{,\eta\eta} & y_{,\eta\eta} \\ x_{,\zeta\eta} & y_{,\zeta\eta} \end{bmatrix} = \begin{bmatrix} 0 & 0 \\ 0 & 0 \\ \dfrac{-\sin(\beta-\alpha)}{L_x\sin(\beta)} & 0 \end{bmatrix}
\tag{8}
$$

$$
\left[j^{(2)}\right] = \begin{bmatrix} (x_{,\zeta})^2 & (y_{,\zeta})^2 & x_{,\zeta}y_{,\zeta} \\ (x_{,\eta})^2 & (y_{,\eta})^2 & x_{,\eta}y_{,\eta} \\ x_{,\zeta}x_{,\eta} & y_{,\zeta}y_{,\eta} & \dfrac{y_{,\eta}x_{,\zeta+y_{,\zeta}x_{,\eta}}}{2} \end{bmatrix}
$$

Using Eqs. (2) and (7), one can obtain the governing equations of motion of moderately thick trapezoidal plate in the $\zeta{-}\eta$ coordinate as:

$$
\begin{aligned}
& k^2A_{55}\left(b_1\frac{\partial \phi_x}{\partial \zeta} + k_{11}\frac{\partial^2 w}{\partial \zeta^2}\right) + k^2A_{44}\left(b_3\frac{\partial \phi_y}{\partial \zeta} + b_4\frac{\partial \phi_y}{\partial \eta} + k_{21}\frac{\partial^2 w}{\partial \zeta^2}\right. \\
& \quad \left. + k_{22}\frac{\partial^2 w}{\partial \eta^2} + k_{23}\frac{\partial^2 w}{\partial \eta \partial \zeta} - a_{21}\frac{\partial w}{\partial \zeta}\right) + k^2A_{45}\left(b_3\frac{\partial \phi_x}{\partial \zeta} + b_4\frac{\partial \phi_x}{\partial \eta}\right) \\
& \quad + k^2A_{45}b_1\frac{\partial \phi_y}{\partial \zeta} + k^2A_{45}\left(k_{31}\frac{\partial^2 w}{\partial \zeta^2} + k_{32}\frac{\partial^2 w}{\partial \eta^2}\right. \\
& \quad \left. + k_{33}\frac{\partial^2 w}{\partial \eta \partial \zeta} - a_{31}\frac{\partial w}{\partial \zeta}\right) = I_0\ddot{w}
\end{aligned}
\tag{9.1}
$$

$$
\begin{aligned}
& D_{11}\left(k_{11}\frac{\partial^2 \phi_x}{\partial \zeta^2}\right) + \frac{(D_{12}+D_{66})}{2}\left(k_{31}\frac{\partial^2 \phi_y}{\partial \zeta^2} + k_{32}\frac{\partial^2 \phi_y}{\partial \eta^2} + k_{33}\frac{\partial^2 \phi_y}{\partial \zeta \partial \eta} - a_{31}\frac{\partial \phi_y}{\partial \zeta}\right) + D_{66}\left(k_{21}\frac{\partial^2 \phi_x}{\partial \zeta^2} + k_{22}\frac{\partial^2 \phi_x}{\partial \eta^2} + k_{23}\frac{\partial^2 \phi_x}{\partial \eta \partial \zeta} - a_{21}\frac{\partial \phi_x}{\partial \zeta}\right) \\
& \quad - k^2A_{55}\left(\phi_x + b_1\frac{\partial w}{\partial \zeta}\right) + D_{16}\left(k_{31}\frac{\partial^2 \phi_x}{\partial \zeta^2} + k_{32}\frac{\partial^2 \phi_x}{\partial \eta^2} + k_{33}\frac{\partial^2 \phi_x}{\partial \eta \partial \zeta} - a_{31}\frac{\partial \phi_x}{\partial \zeta}\right) + D_{16}\left(k_{11}\frac{\partial^2 \phi_y}{\partial \zeta^2}\right) \\
& \quad + D_{26}\left(k_{21}\frac{\partial^2 \phi_y}{\partial \zeta^2} + k_{22}\frac{\partial^2 \phi_y}{\partial \eta^2} + k_{23}\frac{\partial^2 \phi_y}{\partial \zeta \partial \eta} - a_{21}\frac{\partial \phi_y}{\partial \zeta}\right) - k^2A_{45}\left(b_3\frac{\partial w}{\partial \zeta} + b_4\frac{\partial w}{\partial \eta} + \phi_y\right) = I_2\ddot{\phi}_x
\end{aligned}
\tag{9.2}
$$

$$
\begin{aligned}
& D_{66}\left(k_{11}\frac{\partial^2 \phi_y}{\partial \zeta^2}\right) + \frac{(D_{12}+D_{66})}{2}\left(k_{31}\frac{\partial^2 \phi_x}{\partial \zeta^2} + k_{32}\frac{\partial^2 \phi_x}{\partial \eta^2} + k_{33}\frac{\partial^2 \phi_x}{\partial \zeta \partial \eta} - a_{31}\frac{\partial \phi_x}{\partial \zeta}\right) + D_{22}\left(k_{21}\frac{\partial^2 \phi_y}{\partial \zeta^2} + k_{22}\frac{\partial^2 \phi_y}{\partial \eta^2} + k_{23}\frac{\partial^2 \phi_y}{\partial \zeta \partial \eta} - a_{21}\frac{\partial \phi_y}{\partial \zeta}\right) \\
& \quad - k^2A_{44}\left(\phi_y + b_3\frac{\partial w}{\partial \zeta} + b_4\frac{\partial w}{\partial \eta}\right) D_{16}k_{11}\frac{\partial^2 \phi_x}{\partial \zeta^2} + D_{26}\left(k_{21}\frac{\partial^2 \phi_x}{\partial \zeta^2} + k_{22}\frac{\partial^2 \phi_x}{\partial \eta^2} + k_{23}\frac{\partial^2 \phi_x}{\partial \zeta \partial \eta} - a_{21}\frac{\partial \phi_x}{\partial \zeta}\right) \\
& \quad + D_{26}\left(k_{31}\frac{\partial^2 \phi_y}{\partial \zeta^2} + k_{32}\frac{\partial^2 \phi_y}{\partial \eta^2} + k_{33}\frac{\partial^2 \phi_y}{\partial \zeta \partial \eta} - a_{31}\frac{\partial \phi_y}{\partial \zeta}\right) - k^2A_{45}\left(b_1\frac{\partial w}{\partial \zeta} + \phi_x\right) = I_2\ddot{\phi}_y
\end{aligned}
\tag{9.3}
$$

in which:

$$\begin{aligned} &b_1 = [j]^{-1}(1,1) \quad b_3 = [j]^{-1}(2,1) \quad b_4 = [j]^{-1}(2,2) \\ &k_{mn} = \left[j^{(2)}\right]^{-1}(m,n) \quad a_{mn} = \left[j^{(2)}\right]^{-1}\left[j^{(1)}\right][j]^{-1}(m,n) \end{aligned} \tag{10}$$

It should be noted that boundary conditions also can be transformed into the computational domain using Eqs. (4) and (7).

3. Solution procedure

In this section, solution procedure for the governing equations is presented. Differential quadrature (DQ) method, introduced in 1970's, is based on domain discretization for derivation computation. Because of difficulty in weighting coefficient computation, DQ method was ignored by the literature. Generalized DQ method (GDQM) was introduced in order to overcome the problems of DQ method (Shu, 2000). Computation of weighting coefficients is easier in GDQ method. This method is known to be highly accurate even with low computational effort and has been used as an efficient numerical method in structural mechanics analysis (Tornabene and Viola, 2008; Sadeghian and Rezazadeh, 2009). GDQ method uses weighted linear combination of function values in the whole domain to approximate the function derivations with respect to the space variables. For instance, the nth-order derivative of variable V with respect to the ζ at point ζ_i is approximated as:

$$V^{(n)}(\zeta_i) = \left(\frac{d^n V}{d\zeta^n}\right)\bigg|_{\zeta=\zeta_i} = \sum_{j=1}^{N_\zeta} C_\zeta^{(n)}(i,j)V_j, \quad 1 \le i \le N_\zeta \tag{11}$$

where N_ζ is the total number of grid points in the ζ direction and $C_\zeta^{(n)}(i,j)$ are weighting coefficients for the nth-order derivative. In the GDQ method, the global Lagrange interpolation polynomial is used for determination of the weighting coefficients as:

$$g_j(\zeta) = \prod_{k=1,k\neq j}^{N_\zeta} \frac{\zeta-\zeta_k}{\zeta_j-\zeta_k}, \quad 1 \le j \le N_\zeta \tag{12}$$

Eq. (12) can also be written as:

$$\begin{aligned} g_j(\zeta) &= \frac{M(\zeta)}{(\zeta-\zeta_j)M^{(1)}(\zeta_j)} \\ M(\zeta) &= \prod_{k=1}^{N_\zeta}(\zeta-\zeta_k) \\ M^{(1)}(\zeta_j) &= \prod_{k=1,k\neq j}^{N_\zeta}(\zeta_j-\zeta_k) \end{aligned} \tag{13}$$

From Eq. (13), it can be concluded that $M^{(1)}(\zeta)$ is the first derivation of $M(\zeta)$. Now, derivation from Eq. (12) leads to analytic expression for $C_\zeta^{(n)}(i,j)$ as:

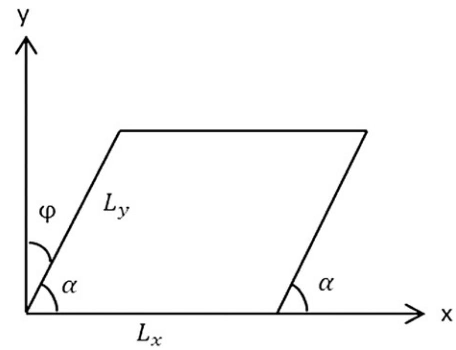

Fig. 2. Schematic figure of skew plate.

$$\begin{aligned} C_\zeta^{(1)}(i,j) &= g_j^{(1)}(\zeta_i), \quad 1 \le i,j \le N_\zeta, i \neq j \\ C_\zeta^{(1)}(i,i) &= -\sum_{j=1,j\neq i}^{N_\zeta} C_\zeta^{(1)}(i,j), \quad 1 \le i \le N_\zeta \end{aligned} \tag{14}$$

The higher order derivative weighting coefficients can be obtained using following recursive formula:

$$\begin{aligned} C_\zeta^{(n)}(i,j) &= n\left(C_\zeta^{(1)}(i,j)C_\zeta^{(n-1)}(i,i) - \frac{C_\zeta^{(n-1)}(i,j)}{\zeta_i-\zeta_j}\right), \ 1 \le i,j \le N_\zeta, i \neq j \\ C_\zeta^{(n)}(i,i) &= -\sum_{j=1,j\neq i}^{N_\zeta} C_\zeta^{(n)}(i,j), \ 1 \le i \le N_\zeta \end{aligned} \tag{15}$$

Using Eq. (11), one may rewrite the governing equations in algebraic discretized form. For example, the discretized form of the first governing equation, Eq. (9.1), can be read as:

$$\begin{aligned} &k^2 A_{55}\left(\sum_{i=1}^{N_\zeta}\left(b_1 C_\zeta^{(1)}\phi_{x_{i,k}} + k_{11}C_\zeta^{(2)}w_{i,k}\right)\right) \\ &+k^2 A_{44}\left[\sum_{i=1}^{N_\zeta}\left(b_3 C_\zeta^{(1)}\phi_{y_{i,k}} + k_{21}C_\zeta^{(2)}w_{i,k} - a_{21}C_\zeta^{(1)}w_{i,k}\right) + \sum_{j=1}^{N_\eta}\left(b_4 C_\eta^{(1)}\phi_{y_{l,j}} + k_{22}C_\eta^{(2)}w_{l,j}\right) + \sum_{m=1}^{N_\zeta}\sum_{n=1}^{N_\eta} k_{23}C_\zeta^{(1)}C_\eta^{(1)}w_{m,n}\right] \\ &+k^2 A_{45}\left[\sum_{i=1}^{N_\zeta}\left(b_3 C_\zeta^{(1)}\phi_{x_{i,k}} + b_1 C_\zeta^{(1)}\phi_{y_{i,k}}\right) + k_{31}C_\zeta^{(2)}w_{i,k} - a_{31}C_\zeta^{(1)}w_{i,k}\right] \\ &+k^2 A_{45}\left[\sum_{j=1}^{N_\eta}\left(b_4 C_\eta^{(1)}\phi_{x_{l,j}} + k_{32}C_\eta^{(2)}w_{l,j}\right)\right] = I_o\ddot{w}; \ l = 2,\ldots,N_\zeta-1, k = 2,\ldots,N_\eta-1 \end{aligned}$$

Table 1
First six dimensionless frequencies of isotropic skew plate $\left(\varpi = \frac{\omega L_y^2}{\pi^2}\sqrt{\frac{\rho h}{D_{11}}}; \frac{L_x}{L_y} = 1; \varphi = 45^\circ\right)$. Increase in thickness results in decrease in frequencies.

B.C.	h/L_y		Modes sequence					
			1st	2nd	3rd	4th	5th	6th
CFCF	0.001	Present	3.6852	3.8432	6.2509	8.7740	10.3352	11.5127
		Liew et al.	3.6933	3.8576	6.2601	8.7946	10.4060	11.5420
		Woo et al.	3.7149	3.8948	6.2744	8.8512	10.6030	–
	0.2	Present	2.5712	2.6307	4.1425	5.2744	5.8359	6.2549
		Liew et al.	2.5674	2.6266	4.1439	5.2627	5.8254	6.2356
		Woo et al.	2.5659	2.6085	4.1383	5.2599	5.8135	–
CFFF	0.1	Present	0.4418	1.0671	2.5104	2.8640	4.5580	5.2232
		Liew et al.	0.4445	1.0678	2.5095	2.8633	4.5547	5.2238
	0.2	Present	0.4212	0.9649	2.1079	2.3903	3.6863	4.1032
		Liew et al.	0.4218	0.9641	2.1033	2.3866	3.6789	4.0953

Table .2
Fundamental frequency of [0 90 90 0] laminated symmetric trapezoidal plate $\left(\varpi = \frac{\omega a^2}{h}\sqrt{\frac{\rho}{E_2}}\right)$

B.C.	h/a	b/a	Present	Haldar and Manna	Gürses et al.
SSSS	0.1	0.8	17.65	17.39	18.41
		0.6	20.64	20.35	20.48
		0.4	24.15	23.91	24.06
		0.2	27.81	27.50	27.54
	0.2	0.8	12.31	11.97	11.99
		0.6	13.88	13.49	13.51
		0.4	15.85	15.44	15.46
		0.2	18.06	17.54	17.63
CCCC	0.1	0.8	25.49	24.73	25.12
		0.6	28.41	27.53	27.62
		0.4	31.95	30.95	31.08
		0.2	35.90	34.74	34.76
	0.2	0.8	15.00	14.46	14.59
		0.6	16.39	15.76	15.88
		0.4	18.14	17.45	17.56
		0.2	20.24	19.45	19.51

Table 3
Convergence study for thin isotropic SSSS skew plate $\left(\varpi = \frac{\omega L_y^2 \sqrt{\rho h / D_{11}}}{\pi^2}\right)$

φ	Method	Modes sequence					
		1st	2nd	3rd	4th	5th	6th
15°	Present 8 × 8	2.1143	4.8931	5.6842	7.9909	10.5903	11.1146
	12 × 12	2.1141	4.8841	5.6838	8.0078	10.5337	11.0276
	16 × 16	2.1143	4.8841	5.6843	8.0084	10.5372	11.0314
	20 × 20	2.1143	4.8841	5.6845	8.0085	10.5372	11.0317
	24 × 24	2.1144	4.8841	5.6846	8.0085	10.5372	11.0319
	McGee et al., 1996	2.1144	4.8842	5.6848	8.0087	10.5370	–
	Bardell,	2.1145	4.8842	5.6850	8.0088	10.5370	11.0330
45°	8 × 8	3.5168	6.7045	10.0863	10.9841	15.4836	18.0795
	12 × 12	3.5119	6.7152	10.1518	10.8569	14.2557	17.0473
	16 × 16	3.5149	6.7152	10.1554	10.8437	14.2658	17.0508
	20 × 20	3.5166	6.7152	10.1558	10.8411	14.2659	17.0509
	24 × 24	3.5175	6.7152	10.1561	10.8408	14.2659	17.0508
	McGee et al., 1996	3.5208	6.7153	10.1570	10.8450	14.2660	–
	Bardell	3.5498	6.7154	10.1660	10.9080	14.2660	17.0510

In the GDQ method, convergence and accuracy of results depend on the distribution of internal nodes. In the most common manner, these nodes are chosen uniformly but investigations show that non-uniform meshes with denser distribution near the boundary lead to more accurate answer (Ng et al., 2009). In this study nodes are chosen according to Chebyshev-Gauss-Lobatto distribution as:

$$\zeta_i = \frac{L_\zeta}{2}\left(1 - \cos\left(\frac{i-1}{N_\zeta - 1}\pi\right)\right) \tag{16}$$

where L_ζ is the length in the ζ direction.

Applying GDQ method on Eq. (9) with the special combination of boundary conditions, one can write the resultant set of algebraic linear equations as:

$$[K]\{q\} = [M]\left\{\frac{\partial^2 q}{\partial t^2}\right\} \tag{17}$$

in which$\{q\}$ is vector of system degree of freedoms including values of w, ϕ_x and ϕ_y at all nodes. In order to obtain the natural frequencies, the nodes on boundaries and internal domain of the plate are separated. Field equations of motion and boundary condition equations can now be rewritten as:

Equations of motion:

$$[[K_{dd}][K_{db}]]\left\{\begin{array}{c} q_d \\ q_b \end{array}\right\} = [M_{dd}]\left\{\frac{\partial^2 q_d}{\partial t^2}\right\} \tag{18.1}$$

Boundary condition equations:

$$[[K_{bd}][K_{bb}]]\left\{\begin{array}{c} q_d \\ q_b \end{array}\right\} = 0 \tag{18.2}$$

Here, subscripts d and b indicate domain and boundary nodes, respectively. For example, $[K_{db}]$ indicates the effects of boundary nodes on the vibration of domain nodes. Combination of Eq (18) leads to:

$$\begin{bmatrix} K_{dd} & K_{db} \\ K_{bd} & K_{bb} \end{bmatrix}\left\{\begin{array}{c} q_d \\ q_b \end{array}\right\} = \begin{bmatrix} M_{dd} & 0 \\ 0 & 0 \end{bmatrix}\left\{\begin{array}{c} \frac{\partial^2 q_d}{\partial t^2} \\ \frac{\partial^2 q_b}{\partial t^2} \end{array}\right\} \tag{19}$$

Due to harmonic nature of the vibration, it is reasonable to assume:

$$q = Q(\zeta, n)e^{i\omega t} \tag{20}$$

where ω is natural frequency of the plate. Substituting Eq. (20) into Eq. (19) together with elimination of boundary nodes, one may rewrite the resultant equation as:

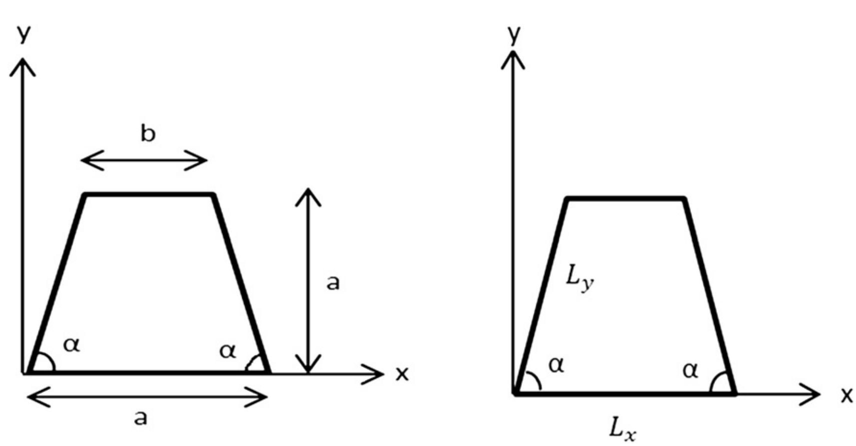

Fig. 3. Schematic view of isosceles (symmetric) trapezoidal plate.

Table 4
The first three dimensionless frequencies for symmetric trapezoidal $\left(h/a = 0.1,\ \bar{\omega} = \frac{\omega a^2\sqrt{\rho/E_2}}{h}\right)$

B.C.	b/a	Lay-up	1st mode	2nd mode	3rd mode
CFCF	0.2	[45 60 60 45]	17.20	29.49	36.70
		[30 60 60 30]	19.54	31.63	39.61
	0.4	[45 60 60 45]	15.74	26.09	32.19
		[30 60 60 30]	18.37	28.24	35.86
	0.6	[45 60 60 45]	14.34	20.80	26.06
		[30 60 60 30]	17.25	24.41	28.13
	0.8	[45 60 60 45]	12.90	15.76	23.25
		[30 60 60 30]	16.18	19.26	23.82
CCFF	0.2	[45 60 60 45]	12.49	22.45	32.15
		[30 60 60 30]	13.51	23.67	33.77
	0.4	[45 60 60 45]	9.84	18.02	27.50
		[30 60 60 30]	11.05	18.69	28.08
	0.6	[45 60 60 45]	7.97	15.50	25.14
		[30 60 60 30]	8.94	15.67	25.53
	0.8	[45 60 60 45]	6.74	13.75	21.87
		[30 60 60 30]	7.35	13.99	23.74
CSFF	0.2	[45 60 60 45]	7.15	17.10	27.51
		[30 60 60 30]	9.52	19.90	30.37
	0.4	[45 60 60 45]	5.94	13.71	22.78
		[30 60 60 30]	8.16	15.83	24.70
	0.6	[45 60 60 45]	4.94	11.59	20.59
		[30 60 60 30]	6.89	12.96	22.16
	0.8	[45 60 60 45]	4.17	10.30	18.90
		[30 60 60 30]	5.81	11.31	20.72

$$\left([K_T] + \omega^2[M_{dd}]\right)\{Q_d\} = 0 \tag{21}$$

in which $[K_T] = [K_{dd}] - [K_{db}][K_{bb}]^{-1}[K_{bd}]$. Solution of this eigenvalue problem results in natural frequencies, ω and mode shape vectors.

4. Results and discussion

In this section, results of the free vibration analyses of symmetrically laminated trapezoidal plates with different boundary conditions and geometrical parameters are presented through some numerical examples. The boundary conditions of the plate are specified by the letter symbols, for example, SCFS means a plate with edges $\zeta = 0$ simply supported (S), $\eta = 0$ clamped (C), $\zeta = L_x$ free (F) and $\eta = L_y$ simply supported (S). In order to validate the present approach, results are compared with some existing ones in the literature.

Table 5
First six dimensionless frequencies for laminated composite [0 90 90 0] with $\alpha = 45°$ $\beta = 120°$ and $L_x = L_y = 1$ $\left(\bar{\omega} = \frac{\omega L_y^2\sqrt{\rho h/D_{11}}}{\pi^2}\right)$

h/L_x	B.C.	1st mode	2nd mode	3rd mode	4th mode	5th mode	6th mode
0.01	CCCC	7.5613	13.7563	14.3517	21.6562	22.8620	23.2259
	SSSS	4.0284	9.1422	9.3679	15.8675	16.7520	17.0625
	CFCF	3.2905	7.4257	7.8596	13.5195	14.3333	14.4388
	SFSF	1.6309	5.1685	5.2248	10.4941	10.9469	11.1020
	CSFF	1.7708	5.2700	6.2908	10.5622	12.2843	12.4914
0.05	CCCC	5.0205	8.0212	8.4070	11.1256	11.9268	12.2236
	SSSS	3.4430	6.7272	7.0769	10.0240	10.9423	11.1950
	CFCF	2.4724	4.9673	5.1502	7.7716	8.3360	8.8741
	SFSF	1.5192	4.1789	4.3261	7.1774	7.8347	8.1975
	CSFF	1.8318	4.3037	4.8898	7.6468	8.1599	8.7973
0.1	CCCC	3.1504	4.7519	5.0527	6.3422	6.8443	7.1554
	SSSS	2.5831	4.3701	4.7636	6.0299	6.6654	6.9823
	CFCF	1.6811	3.1006	3.3667	4.5977	5.0930	5.5913
	SFSF	1.2821	2.8908	3.1781	4.4410	5.0321	5.4618
	CSFF	1.4895	3.0124	3.4376	4.8982	5.2045	5.7027
0.15	CCCC	2.2451	3.3235	3.5598	4.3761	4.7414	5.0085
	SSSS	1.9853	3.1527	3.4726	4.2366	4.8935	4.9541
	CFCF	1.2551	2.2418	2.4737	3.2396	3.6474	3.9842
	SFSF	1.0685	2.2278	2.3184	3.1230	3.8327	3.8460
	CSFF	1.1915	2.2780	2.5774	3.5089	3.7589	4.1268
0.2	CCCC	1.7311	2.5592	3.1842	3.6903	3.7636	3.8477
	SSSS	1.5891	2.4405	2.8736	3.4312	3.8300	5.0472
	CFCF	1.0081	1.8195	2.0555	2.1168	2.9054	3.0591
	SFSF	0.7563	0.8849	1.6013	1.6169	2.8092	3.0895
	CSFF	0.9761	1.8421	2.0443	2.7989	3.0228	3.5741

The first example is an isotropic skew plate as shown in Fig. 2 with the $L_x = L_y = 1$ and $\phi = 45°$. Dimensionless natural frequency of the skew plate is presented in Table 1. Results of FEM (Woo et al., 2003) and Ritz method (Liew et al., 1993) are also included in the table for comparison. It can be concluded from the table that predictions of the GDQ method are in good agreement with the FEM and specially the semi-analytical results of Ritz method presented by Liew et al. as the maximum relative discrepancy between the GDQ and Ritz results is about 0.6% and the average discrepancy is 0.19%. Note that a mesh size of 12 × 12 is used to obtain solutions for the GDQ method.

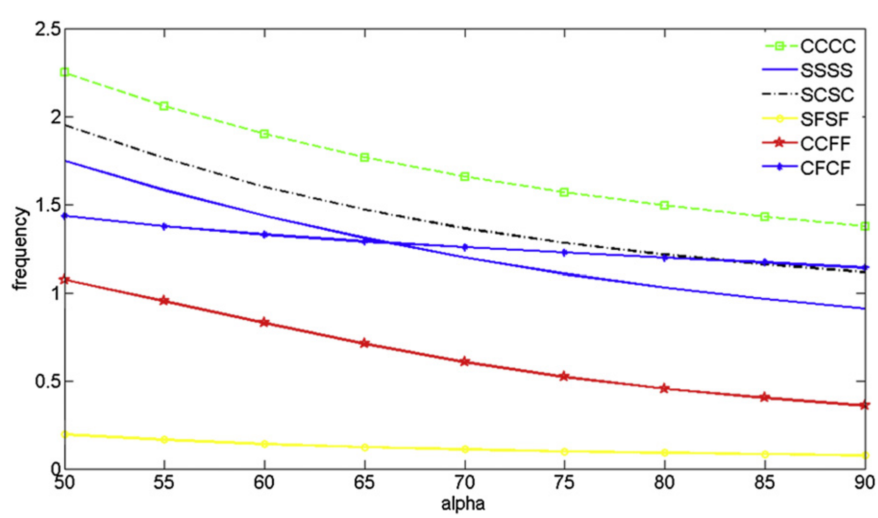

Fig. 4. Fundamental natural frequency of [0 90 90 0] laminated symmetric trapezoidal plate $\left(\bar{\omega} = \omega L_y^2\sqrt{\frac{\rho h}{D_{11}}} L_x = L_y = 1 \text{ and } h/L_y = 0.1.\right)$

Table 6
Dimensionless frequencies for right trapezoidal with $L_x = 1$, $L_y = 0.5$ and $h = 0.1\ L_y$. $\left(\overline{\omega} = \dfrac{\omega L_y^2 \sqrt{\rho/E_2}}{h}\right)$

θ	B.C.	Lay-up	1st mode	2nd mode	3rd mode
45°	CCCC	[0 90 90 0]	17.8681	28.1739	33.1729
		[30 60 60 30]	16.8660	23.6182	30.1991
	SSSS	[0 90 90 0]	10.8137	22.7508	26.2021
		[30 60 60 30]	11.7158	19.1542	26.3149
	CSCS	[0 90 90 0]	14.2132	24.8717	28.3264
		[30 60 60 30]	14.8882	21.1920	27.7644
	CFCF'	[0 90 90 0]	9.3864	15.5454	19.2360
		[30 60 60 30]	8.5539	13.7015	15.0513
	SFSF	[0 90 90 0]	5.4563	11.2542	16.0392
		[30 60 60 30]	4.1514	8.6176	9.8155
	CFSF	[0 90 90 0]	7.2436	13.5562	17.5084
		[30 60 60 30]	4.4120	10.1717	13.3471
	CFFF	[0 90 90 0]	1.9660	3.9440	8.7862
		[30 60 60 30]	0.5721	3.3197	5.2285
60°	CCCC	[0 90 90 0]	16.0475	24.4102	31.4960
		[30 60 60 30]	14.7229	20.6923	27.0137
	SSSS	[0 90 90 0]	9.0424	19.1826	24.4781
		[30 60 60 30]	9.8423	16.6872	23.4642
	CSCS	[0 90 90 0]	12.6384	22.1702	28.1801
		[30 60 60 30]	11.8857	18.6075	25.0228
	CFCF	[0 90 90 0]	4.2014	12.0503	14.6134
		[30 60 60 30]	6.9243	8.5822	12.8723
	SFSF	[0 90 90 0]	0.8297	8.7732	11.2317
		[30 60 60 30]	3.4437	4.8424	8.5863
	CFSF	[0 90 90 0]	2.4750	9.9134	12.2810
		[30 60 60 30]	3.7408	7.5853	9.9605
	CFFF	[0 90 90 0]	1.7930	2.7926	8.6196
		[30 60 60 30]	0.6005	2.8582	4.7893
75°	CCCC	[0 90 90 0]	15.2722	22.3134	31.0093
		[30 60 60 30]	13.8648	18.7958	24.9205
	SSSS	[0 90 90 0]	8.3187	16.8817	24.0410
		[30 60 60 30]	9.0712	14.9445	21.6066
	CSCS	[0 90 90 0]	11.7244	19.6856	27.6531
		[30 60 60 30]	10.4675	16.8271	23.1179
	CFCF	[0 90 90 0]	3.4755	9.9512	13.9449
		[30 60 60 30]	5.6098	6.6965	11.9121
	SFSF	[0 90 90 0]	0.7479	7.5459	10.5060
		[30 60 60 30]	2.8917	3.5692	8.0107
	CFSF	[0 90 90 0]	1.9820	9.1835	10.8338
		[30 60 60 30]	3.2713	5.7610	9.3811
	CFFF	[0 90 90 0]	1.6273	2.3026	8.3163
		[30 60 60 30]	0.6356	2.5571	4.4995

The other verification example is a symmetrically laminated isosceles trapezoidal plate, see Fig. 3. Composite material properties used in this study are as:

$$E_1 = 40E_2,\ G = 0.6E_2,\ \vartheta_{12} = 0.25,\ \rho = 2500\ \mathrm{Kg/m^3}$$

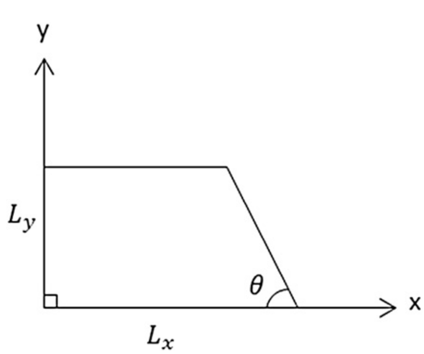

Fig. 5. Right trapezoidal plate.

Dimensionless fundamental natural frequency of SSSS and CCCC trapezoidal plate for different values of b/a and h/a are presented in Table 2. In this table, results of some previous studies are also included for comparison. Again, a good agreement can be seen between results of the GDQ method and those available from FEM and DSC method as the predicted frequency for a SSSS plate with $h/a = 0.1$ and $b/a = 0.2$ is 27.81 that shows 1.1% and 0.9% error with respect to FEM and DSC method results respectively.

In Table 3, convergence of the GDQ method for the first six dimensionless natural frequencies of isotropic SSSS skew plate shown in Fig. 2. with $L_x = L_y = 1$ and $h/L_x = 0.001$ is investigated. Results are prepared for two different values of skew angle. The problem is solved with five different mesh sizes. Results of the analytical solution (McGee et al., 1996) and FEM (Bardell, 1992) are also included for comparison. From the results one can conclude that GDQ leads to accurate results even using a few grid points. For instance, with mesh size of 8×8 and 12×12 forth dimensionless natural frequency of skew plate with skew angle $\varphi = 15°$ is obtained as 7.9909 and 8.0078, respectively which shows 0.22% and 0.01% difference with analytical results. Furthermore, results show that as the number of grid points increased GDQ results are rapidly converged to the final values which show fast rate of convergence of the method. Thus, the mesh size of 12×12 is used in the next numerical examples.

Effect of geometrical parameters and lay-up configuration on the natural frequency of symmetric trapezoidal, see Fig. 3.with free edge is studied in Table 4. In this table, the first three natural frequencies of the trapezoidal plate are prepared for different values of $\dfrac{b}{a}$ and different lay-up configurations. From these results one can conclude that as the $\dfrac{b}{a}$ increases and the plate tends to the rectangular shape, dimensionless natural frequencies decrease.

Effect of the boundary conditions on the fundamental natural frequency of trapezoidal plates, shown in Fig. 3, is presented in Fig. 4. In this figure, fundamental frequency of a [0 90 90 0] plate versus α is presented for different sets of boundary conditions. Again, it can be concluded that as the plate tends to the rectangular shape ($\alpha = 90°$), natural frequency decreases gradually. It might be due to the fact that by approaching to the rectangle shape, stress singularity near the corners of trapezoidal plates reduces.

Table 5 shows the first six dimensionless frequencies of general trapezoidal plate (Fig. 1.) for various boundary conditions and different values of thickness. Results show that as the plate thickness increased, natural frequencies are decreased.

Table 6 shows the first three dimensionless natural frequencies of a moderately thick right trapezoidal (Fig. 5.) with different geometrical parameters, boundary conditions and lay-up configurations. Results show that as the angle θ increased, dimensionless frequency decreased.

In this study, free vibration of symmetrically laminated trapezoidal plates with various boundary conditions is investigated using GDQ method. As special case of trapezoidal plates one can refer to the triangular plates by limiting upper edge length to the zero, see Fig. 6. In order to study the applicability of the presented solution to the triangle shape, equilateral triangle is built by approaching α to the 60° and holding $L_y = L_x = 1$.

Dimensionless fundamental natural frequency of symmetrically laminated triangular plates obtained based on the GDQM for different values of α together with ANSYS results are presented in Table 7. In this table results are prepared for different values of plate thickness and lay-up configurations. Results show that as the value of α tends to 60°, difference between the GDQ predictions and ANSYS

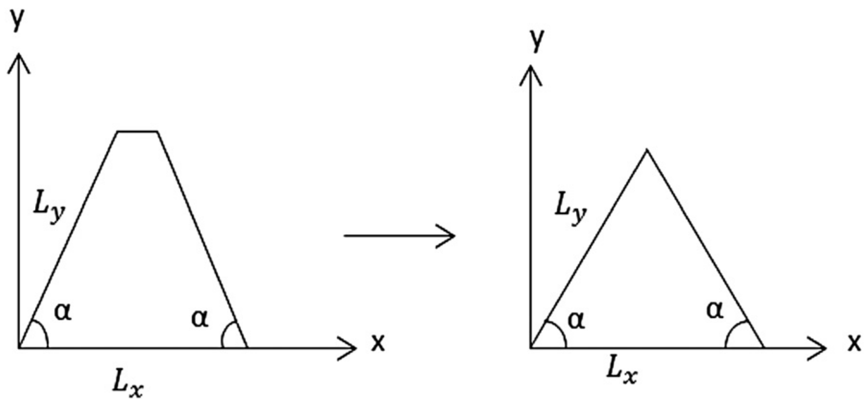

Fig. 6. Equilateral triangle as a special case of trapezoidal by limiting upper edge length to the zero and holding $L_x = L_y = 1$.

Table 7
Fundamental dimensionless frequency for fully clamped symmetric triangle $\left(L_x = L_y, \ \overline{\omega} = \dfrac{\omega L_y^2 \sqrt{\rho / E_2}}{h}\right)$.

h/a	Lay-up	Present			ANSYS
		$\alpha = 61^\circ$	$\alpha = 60.5^\circ$	$\alpha = 60.05$	
0.05	[0 90 90 0]	66.51	67.33	68.17	70.61
	[30 60 60 30]	57.68	58.45	59.18	59.28
	[45 60 60 45]	55.43	56.28	57.13	56.21
	[30 90 90 30]	62.94	63.82	64.54	65.16
0.1	[0 90 90 0]	42.41	42.91	43.32	44.44
	[30 60 60 30]	37.49	37.94	38.39	39.07
	[45 60 60 45]	36.25	36.73	37.12	37.60
	[30 90 90 0]	40.67	41.19	41.61	42.07
0.15	[0 90 90 0]	28.85	29.17	31.17	31.78
	[30 60 60 30]	27.70	28.02	29.18	29.02
	[45 60 60 45]	27.26	27.23	27.49	28.15
	[30 90 90 30]	29.64	30.00	30.20	30.62

results decreases. It is worth mentioning that since the solution procedure is based on the general trapezoidal plate it is impossible to set $\alpha = 60^\circ$. Furthermore, an increase in the plate thickness causes decrease in the dimensionless natural frequencies.

5. Conclusions

Free vibration analysis of moderately thick symmetrically laminated trapezoidal, skew and triangle plates with various boundary conditions is investigated. The existing governing equations of the problem based on the FSDT in the Cartesian coordinate system are properly transformed into trapezoidal coordinate. The GDQ method is used for discretizing of governing equations. Results of the present study are compared with available results in the literature. Effects of different parameters such as geometrical parameters, lay-up configurations and boundary conditions on the dynamic behavior of the trapezoidal, skew and triangle plates are presented. The results show that by increasing the thickness, the dimensionless frequencies of trapezoidal plate decrease. Furthermore, by tending to a rectangular plate, the dimensionless frequency of the trapezoidal plate decreases gradually.

References

Bardell, N.S., 1992. The free vibration of skew plates using the hierarchical finite element method. Comput. Struct. 45, 841–874.

Chen, C.C., Kitipornchai, S., Lim, C.W., Liew, K.M., 1999. Free vibration of cantilevered symmetrically laminated thick trapezoidal plates. Int. J. Mech. Sci. 41, 685–702.

Dozio, L., Carrera, E., 2011. A variable kinematic Ritz formulation for vibration study of quadrilateral plates with arbitrary thickness. J. Sound Vib. 330, 4611–4632.

Fallah, A., Kargarnivin, M.H., Aghdam, M.M., 2011. Free vibration analysis of symmetrically Laminated Fully Clamped skew plate using extended Kantorovich method. Key Eng. Mater. 471-472, 739–744.

Ferreira, A.J.M., Roque, C.M.C., Jorge, R.M.N., 2005. Free vibration analysis of symmetric laminated composite plates by FSDT and radial basis functions. Comput. Methods Appl. Mech. Eng. 194, 4265–4278.

Ferreira, A.J.M., Roque, C.M.C., Carrera, E., Cinefra, M., 2011. Analysis of thick isotropic and cross-ply laminated plates by radial basis functions and a Unified Formulation. J. Sound Vib 330, 771–787.

Gürses, M., Civalek, O., Ersoy, H., Kiracioglu, O., 2009. Analysis of shear deformable laminated composite trapezoidal plates. Mater. Des. 30, 3030–3035.

Haldar, S., Manna, M.C., 2003. A high precision shear deformable element for free vibration of thick/thin composite trapezoidal plates. Steel Compos. Struct. 3 (3), 213–229.

Kang, W., Lee, N.H., Pang, S., Chung, W.Y., 2005. Approximate closed form solution for free vibration of polar orthotropic circular plates. Appl. Acoust. 66 (10), 1162–1179.

Khdeir, A.A., 1988. Free vibration and buckling of symmetric cross-ply laminated plates by an exact method. J. Sound Vib. 126 (3), 447–461.

Kitipornchni, S., Xiang, Y., Liew, K.M., Lim, M.K., 1994. A global approach for vibration of thick trapezoidal plates. Comput. Struct. 53, 83–92.

Liew, K.M., 1992. Vibration of symmetrically laminated cantilever trapezoidal composite plate. Int. J. Mech. Sci. 34, 299–308.

Liew, K.M., Haung, Y.Q., 2003. Bending and buckling of thick symmetric rectangular laminates using the moving least-square differential quadrature method. Int. J. Mech. Sci. 45, 95–114.

Liew, K.M., Lam, K.Y., 1991. A Rayleigh-Ritz approach to transverse vibration of isotropic and anisotropic trapezoidal plate using orthogonal plate functions. Int. J. Solids Struct. 27, 189–203.

Liew, K.M., Xiang, Y., Kitipomchai, S., Wang, C.M., 1993. Vibration of thick skew plates based on Mindlin shear deformation plate theory. J. Sound Vib. 168, 39–69.

Liew, K.M., Hung, K.C., Lim, M.K., 1995. Vibration Characteristics of simply supported thick skew plates in three-dimensional setting. J. Appl. Mech. 62, 880–886.

Malekzadeh, P., Karami, G., 2005. Polynomial and harmonic differential quadrature methods for free vibration of variable thickness skew plate. Eng. Struct. 27, 1563–1574.

McGee, O.G., Butalia, T.S., 1992. Natural vibration of shear deformable cantilevered skewed trapezoidal and triangle thick plate. Comput. Struct. 45, 1033–1059.

McGee, O.G., Kim, J.W., Kim, Y.S., 1996. Corner stress singularity effects on the vibration of rhombic plates with combinations of clamped and simply supported edges. J. Sound Vib. 193 (13), 555–580.

Ng, S.S.F., Das, B., 1986. Free vibration and buckling analysis of clamped skew sandwich plates by the Galerkin method. J. Sound Vib. 107, 97–106.

Ng, C.H.W., Zhao, Y.B., Xiang, Y., Wei, G.W., 2009. On the accuracy and stability of a variety of differential quadrature formulation for the vibration analysis of beams. Int. J. Eng. Appl. Sci. 1, 1–25.

Qatu, M.S., 1994. Natural frequencies for cantilevered laminated composite right triangular and trapezoidal plates. Compos. Sci. Technol. 51, 441–449.

Rajalingham, C., Bhat, R.B., Xistris, G.D., 1996. Vibration of rectangular plates using plate characteristic functions as shape function in the Rayleigh-Ritz method. J. Sound Vib. 193 (2), 497–509.

Rao, K.M., Meyer Piening, H.R., 1990. Analysis of thick laminated anisotropic composite plates by finite element method. Compos. Struct. 15, 185–213.

Reddy, J.N., 1997. Mechanics of Laminated Composite Plates and Shells: Theory and Analysis, second ed. CRC Press, New York.

Sadeghian, H., Rezazadeh, G., 2009. Comparison of generalized differential quadrature and Galerkin methods for the analysis of micro-electro-mechanical coupled systems. Commun. Nonlinear Sci. Numer. Simul. 14, 2807–2816.

Shu, C., 2000. Differential Quadrature and Its Applications in Engineering, first ed. Springer, London.

Tornabene, F., Viola, E., 2008. 2-D solution for free vibrations of parabolic shells using generalized differential quadrature method. Eur. J. Mechanics A/Solids 27, 1001–1025.
Woo, K.S., Hong, C.H., Basu, P.K., Seo, C.G., 2003. Free vibration of skew Mindlin plates by p-version of F. E. M. J. Sound Vib. 268, 637–656.
Xiang, Y., 2002. Exact vibration solution for circular Mindlin plate with multiple concentric ring support. Int. J. Solids Struct. 39 (25), 6081–6102.
Yalcin, H.S., Arikoglu, A., Ozkol, I., 2009. Free vibration analysis of circular plates by differential transformation method. Appl. Math. Comput. 212 (2), 377–386.
Zhou, D., Au, F.T.K., Cheung, Y.K., Lo, S.H., 2003. Three-dimensional vibration analysis of circular and annular plates via the Chebyshev-Ritz method. Int. J. Solids Struct. 40 (12), 3089–3105.
Zhou, D., Liu, W., Yang, Q., 2008. Three-dimensional analysis of cantilevered skew plates. J. Sound Vib. 313, 134–148.